QED effects and Photon PDF in the CTEQ-TEA Global Analysis

Carl Schmidt[*]**, Jon Pumplin, Daniel Stump, and C.-P. Yuan**

Department of Physics and Astronomy, Michigan State University, East Lansing, MI 48824 USA
E-mail: schmidt@pa.msu.edu

We describe the implementation of Quantum Electrodynamic (QED) evolution, including a photon Parton Distribution Function (PDF) in the CTEQ-TEA Global analysis package. Constraints are obtained on the photon PDF by comparing with ZEUS data on the production of isolated photons in deep inelastic scattering, $ep \rightarrow e\gamma + X$. The theoretical calculation of this process is described. Comparison with the data gives a constraint on the initial momentum fraction of the photon of $p_0^\gamma \lesssim 0.14\%$ at the 90% confidence level for our parametrization.

[*]Speaker.

The CTEQ-TEA group is currently in the process of updating the CT10 PDFs [1] to include constraints from LHC data. In addition, we have recently included QED effects into our global analysis program. I will focus on this latter subject in this talk. We have included QED evolution at leading order (LO) with next-to-leading order (NLO) QCD evolution in our package [2]. Past studies of QED effects in global analysis have been done by the MRST [3] and the NNPDF [4] groups. We have checked our code against other QED+QCD evolution codes [5, 6, 7] and find good agreement.

The MRST and NNPDF analyses used different approaches for modeling the photon PDF. The MRST group used a parametrization for the photon PDF based on radiation off of "primordial" up and down quarks, cut off by constituent or current quark masses. The NNPDF group used a general photon parametrization, which was then constrained by high energy W, Z and Drell-Yan data at the LHC. In our work we use a generalization of the MRST approach, which we then constrain by Deep Inelastic Scattering with isolated photon data from the ZEUS collaboration [8]. Our photon parametrization at the initial scale $Q_0 = 1.295$ GeV is

$$f_{\gamma/p}(x, Q_0) \;=\; \frac{\alpha}{2\pi} \left(A_u e_u^2 \tilde{P}_{\gamma q} \circ u^0(x) + A_d e_d^2 \tilde{P}_{\gamma q} \circ d^0(x) \right) \;, \tag{1}$$

where $\tilde{P}_{\gamma q} \circ f^0(x)$ is the convolution of the quark-to-photon splitting function $\tilde{P}_{\gamma q}(x)$ with the "primordial" quark distribution $f^0(x)$, which we take to be the initial up and down valence distributions. We then set $A_u = A_d$ to obtain a single parameter family of photon distributions, which we can label by their initial momentum fraction p_γ^0. For comparison, in analogy with the MRST approach, we also consider a "Current Mass" (CM) photon distribution, given by setting $A_i = \ln\left(Q_0^2/m_i^2\right)$, where $i = u, d$, and $m_u = 6$ MeV and $m_d = 10$ MeV are the quark current masses.
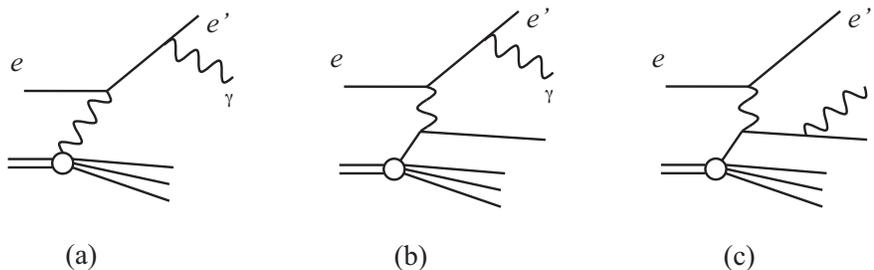

Figure 1: Amplitudes for the process $ep \rightarrow e\gamma + X$. For each diagram shown there is an additional diagram where the photon is emitted off the initial-state lepton or quark.

The constraints on the photon PDF from the DIS and Tevatron data, used in the CT10 analysis are relatively weak, allowing a photon momentum fraction of about 5%. Thus, we are led to consider the process $ep \rightarrow ep + X$, for which the photon PDF contributes at LO with no dominating quark PDF contributions, except those compensated by an extra factor of α. We display the relevant amplitudes in Fig. 1. Previous theoretical calculations of this process have included only the photon-initiated contribution (MRST [3]) of Fig. 1(a) or the quark-initiated contributions (GGP [9, 10]) of Figs. 1(b) and (c). We have performed a new calculation, which consistently combines all the terms in Fig. 1 by treating it as NLO in α, but discarding contributions suppressed by both the photon PDF and an extra factor of α. In particular, using the $\overline{\text{MS}}$ scheme, we factorize

the initial-state collinear singularity in Fig. 1(b) into the definition of the photon PDF, resulting in perfectly well-defined and finite calculation in four dimensions. Following GGP, we find it useful to describe the separate components of the calculation coming from the square of amplitudes with photon-emission off the lepton lines (*LL*, Figs. 1(a) and (b)) and off the quark lines (*QQ*, Fig. 1(c)), and the interference terms (*QL*), which are negligible but still included.

The ZEUS collaboration enforced the following kinematic cuts on their data. Cuts on the photon transverse energy and pseudo rapidity were $4\,\text{GeV} < E_{\perp\gamma} < 15\,\text{GeV}$ and $-0.7 < \eta_\gamma < 0.9$. Cuts on the lepton energy, scattering angle, and momentum transfer were $E'_\ell > 10\,\text{GeV}$, $139.8° < \theta'_\ell < 171.8°$, and $10\,\text{GeV}^2 < Q^2 < 350\,\text{GeV}^2$. A reconstructed track, well separated from the lepton, was required to remove deeply virtual Compton scattering events. Finally, an isolation cut on the photon was enforced, requiring that the photon carried 90% of the energy in the jet (of size $R = 1$) in which it was contained. Theoretically, we handled this isolation cut in two ways. In the sharp isolation prescription we translated this cut directly to the parton level, using the ALEPH LO fragmentation function [11] and associated subtraction to deal with the final-state photon-quark collinear singularity. In the smooth isolation prescription we approximated the isolation cut at the parton level by requiring $E_q < (E_\gamma/9)(1 - \cos r)/(1 - \cos R)$ for cone sizes of $r < R$. This prescription removes all final-state collinear singularities, as well as any dependence on the fragmentation function [12].

In Fig. 2 we display representative plots of the dependence on the factorization scale μ_F for distributions in the photon variables $E_{\perp\gamma}$ and η_γ, separating out the contributions from the different components. From this we see that the scale dependence of the full *LL* component has reduced dramatically compared to the photon-initiated contribution alone. We also see that the *QQ* and *LL* components dominate in different kinematic regions, with the *LL* dominating at large $E_{\perp\gamma}$ and small η_γ. This is useful for constraining the photon PDF. Finally, we note that the scale dependence in the *QQ* component, and therefore in the total prediction, is still large due to the fact that the calculation is LO in α_s.
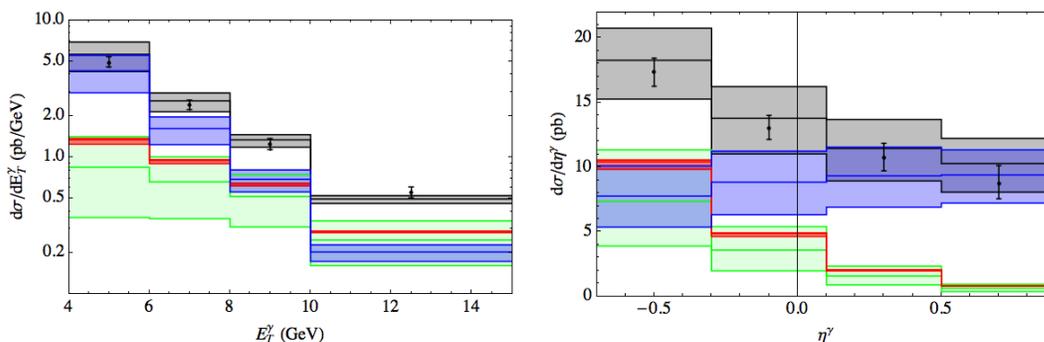

Figure 2: Differential distributions for a zero initial photon PDF and using the smooth isolation prescription. The various bands display a variation in factorization scale between $0.5E_{\perp\gamma} \leq \mu_F \leq 2E_{\perp\gamma}$ and correspond to the total prediction (gray), the *QQ* component (blue), the *LL* component (red), and the photon-initiated contribution only (green). Also shown are the ZEUS data points.

In Fig. 3 we compare predictions from the two different isolation prescriptions. We note that the difference between the predictions is about the same size as the scale uncertainty. In addition,

we find the prediction with smooth isolation is uniformly larger than that with the sharp isolation, in contrast to expectations. Considering that calculations in both prescriptions may be affected by additional QCD radiation, we take the difference between the two prescriptions, as well as the factorization scale dependence, as a measure of the theoretical uncertainty of the calculations.
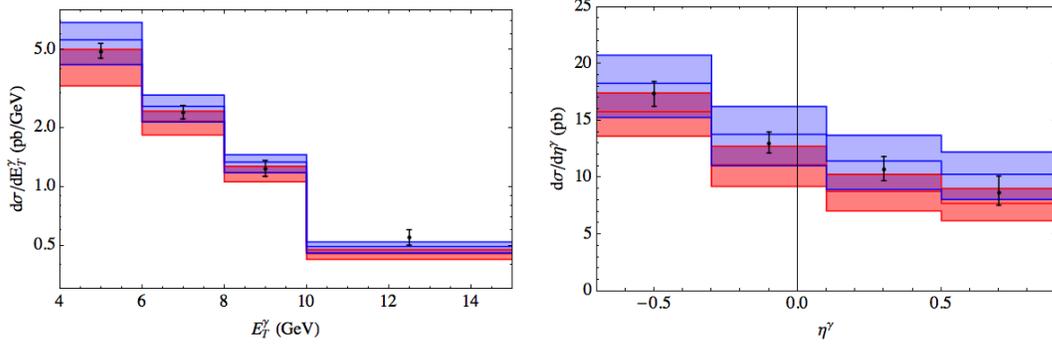

Figure 3: Differential distributions for a zero initial photon PDF with the factorization scale varied between $0.5E_{\perp\gamma} \leq \mu_F \leq 2E_{\perp\gamma}$. The blue band is calculated using the smooth isolation prescription and the red band is calculated using the sharp isolation prescription. Also shown are the ZEUS data points.

In Fig. 4 we compare the ZEUS data with the differential cross sections for several different initial photon PDFs for $\mu_F = 0.5E_{\perp\gamma}$ and with the smooth isolation prescription. Here we see that the differences in shape of the predictions can distinguish between different initial photon PDFs. The photon PDF with $p_0^\gamma = 0.1\%$ fits these data well, but the CM photon fits poorly for these theoretical choices. For completeness, we note that the ZEUS collaboration also plots distributions in the lepton variables Q^2 and x, but due to the kinematic cuts applied, we have found these distributions to be much more sensitive to higher-order QCD radiation. As a consequence, the theory, at least to the order we have calculated, cannot fit the lepton distributions for any choice of photon PDF. Therefore, we only consider the photon distributions in constraining the photon PDF.
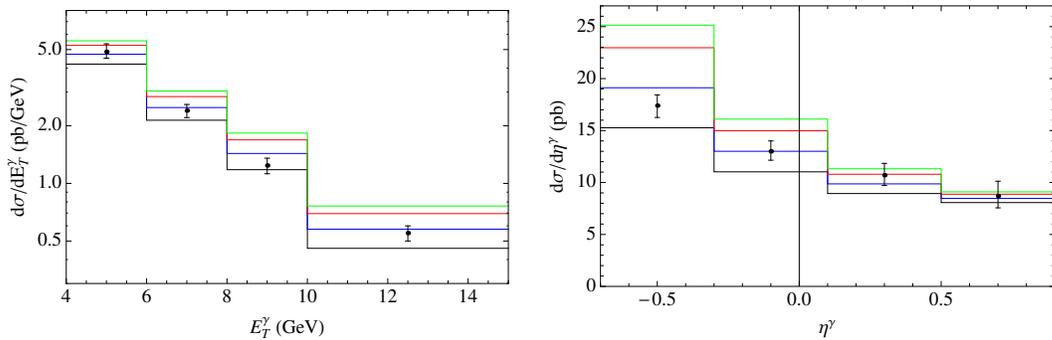

Figure 4: Differential distributions in the photon variables, $E_{\perp\gamma}$ and η_γ, with the smooth isolation prescription, with factorization scale $\mu_F = 0.5E_{\perp\gamma}$. The curves, from bottom to top are with initial photon momentum fractions of $p_0^\gamma = 0\%$ (black), 0.1% (blue), 0.2% (red), and for the CM photon (green). Also shown are the ZEUS data points with combined statistical and systematic errors.

In Fig. 5 we plot the χ^2 for the data points in these two distributions as a function of the initial photon momentum fraction p_0^γ, for both isolation prescriptions and for several different scale choices. Using the fact that $\chi^2 < 13.36$ at the 90% confidence level for 8 data points, we obtain the constraint that $p_0^\gamma \lesssim 0.14\%$ for our one-parameter photon PDF ansatz, independent of isolation prescription or scale choice. In addition, we find that the CM photon PDF has $\chi^2 > 47$ for any choice of isolation and factorization scale and so is ruled out by this data.
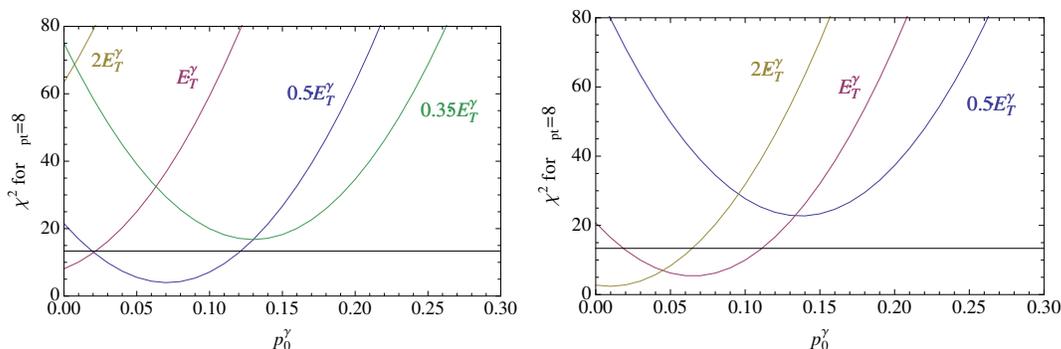

Figure 5: Plots of χ^2 versus initial photon momentum fraction p_0^γ using the smooth isolation prescription (left) and the sharp isolation prescription (right) for factorization scales $\mu_F = 2E_{\perp\gamma}$, $E_{\perp\gamma}$, $0.5E_{\perp\gamma}$, and $0.35E_{\perp\gamma}$.

References

[1] Jun Gao, Marco Guzzi, Joey Huston, Hung-Liang Lai, Zhao Li, Pavel Nadolsky, Jon Pumplin, Daniel Stump, C.-P. Yuan, arXiv:1302.6246 [hep-ph].

[2] C. Schmidt, J. Pumplin, D. Stump, C. -P. Yuan, In preparation.

[3] A. D. Martin, R. G. Roberts, W. J. Stirling and R. S. Thorne, Eur. Phys. J. C **39**, 155 (2005) [hep-ph/0411040].

[4] R. D. Ball *et al.* [NNPDF Collaboration], Nucl. Phys. B **877**, 290 (2013) [arXiv:1308.0598 [hep-ph]].

[5] M. Roth and S. Weinzierl, Phys. Lett. B **590**, 190 (2004) [hep-ph/0403200].

[6] V. Bertone, S. Carrazza and J. Rojo, Comput. Phys. Commun. **185**, 1647 (2014) [arXiv:1310.1394 [hep-ph]].

[7] R. Sadykov, arXiv:1401.1133 [hep-ph].

[8] S. Chekanov *et al.* [ZEUS Collaboration], Phys. Lett. B **687**, 16 (2010) [arXiv:0909.4223 [hep-ex]].

[9] A. Gehrmann-De Ridder, T. Gehrmann and E. Poulsen, Phys. Rev. Lett. **96**, 132002 (2006) [hep-ph/0601073].

[10] A. Gehrmann-De Ridder, T. Gehrmann and E. Poulsen, Eur. Phys. J. C **47**, 395 (2006) [hep-ph/0604030].

[11] D. Buskulic *et al.* [ALEPH Collaboration], Z. Phys. C **69**, 365 (1996).

[12] S. Frixione, Phys. Lett. B **429**, 369 (1998) [hep-ph/9801442].